How to cite: *Angew. Chem. Int. Ed.* **2023**, *62*, e202312521
doi.org/10.1002/anie.202312521

Raman Spectroscopy

Combination of Resonance and Non-Resonance Chiral Raman Scattering in a Cobalt(III) Complex

*Qin Yang, Julien Bloino, Hana Šestáková, Jaroslav Šebestík, Jiří Kessler, Jana Hudecová, Josef Kapitán, and Petr Bouř**

Abstract: Resonance Raman optical activity (RROA) spectra with high sensitivity reveal details on molecular structure, chirality, and excited electronic properties. Despite the difficulty of the measurements, the recorded data for the Co(III) complex with *S,S*-*N,N*-ethylenediaminedisuccinic acid are of exceptional quality and, coupled with the theory, spectacularly document the molecular behavior in resonance. This includes a huge enhancement of the chiral scattering, contribution of the antisymmetric polarizabilities to the signal, and the Herzberg-Teller effect significantly shaping the spectra. The chiral component is by about one order of magnitude bigger than for an analogous aluminum complex. The band assignment and intensity profile were confirmed by simulations based on density functional and vibronic theories. The resonance was attributed to the $S_0 \rightarrow S_3$ transition, with the strongest signal enhancement of Raman and ROA spectral bands below about 800 cm^{-1}. For higher wavenumbers, other excited electronic states contribute to the scattering in a less resonant way. RROA spectroscopy thus appears as a unique tool to study the structure and electronic states of absorbing molecules in analytical chemistry, biology, and material science.

[*] Dr. Q. Yang, H. Šestáková, Dr. J. Šebestík, Dr. J. Kessler, Prof. P. Bouř
Institute of Organic Chemistry and Biochemistry Academy of Sciences
Flemingovo náměstí 2, 16610, Prague (Czech Republic)
E-mail: bour@uochb.cas.cz

Prof. J. Bloino
Scuola Normale Superiore di Pisa
Piazza dei Cavalieri 7, 56126 Pisa (Italy)

H. Šestáková, Prof. P. Bouř
University of Chemistry and Technology
Technická 5, 16628 Prague 6 (Czech Republic)

Dr. J. Hudecová, Dr. J. Kapitán
Department of Optics
Palacký University Olomouc
17. listopadu 12, 77146, Olomouc (Czech Republic)

Molecular Raman scattering has been first observed on colorless liquids, such as toluene,[1] and developed into a powerful tool of contemporary chemistry, physics, and biology.[2] In the 1970s, differences in the scattering of the right and left circularly polarized light could be detected,[3] which provided chiral discrimination and increased the sensitivity to the molecular structure.[4] Following theoretical[5] and instrumental[6] developments, since about 2005, the spectroscopy of Raman optical activity (ROA) has been commercially available. Combined with *a priori* methods to simulate the spectra, it delivers unique information about the structure and behavior of sugars, peptides, proteins, and even whole viruses.[7]

Unfortunately, for transparent samples, the efficiency of Raman scattering and the sensitivity of the technique are rather low. In addition, the differential scattering of ROA is only a small part of the total signal ($\Delta I/I \approx 10^{-4}$).[8] For samples absorbing the excitation light, the signal is often much stronger. In this case of so called resonance Raman[9] or ROA (RROA),[10] the energy of the incident light matches one or more electronic transitions. This allows probing not only molecular geometry, but also the electronic wave function.

On the other hand, the resonance causes many experimental problems, such as sample heating, decomposition, and masking off the Raman effect by fluorescence. Nevertheless, several RROA experiments were reported.[4,11] In parallel, theoretical works have tried to rationalize the origin of the system, for instance with the single electronic state (SES) model connecting RROA intensities with electronic circular dichroism (ECD).[12] Later, it was recognized that ECD combined with polarized Raman scattering can contribute to the measured "RROA" signal.[13] Only when an accurate way to subtract this ECD-Raman interference was found the full power of RROA could be unleashed.[13a,14]

Interpretation and simulations of the resonance spectra are difficult as well. In the simplest SES approximation, the RROA spectrum is just proportional to the Raman one.[12] In general, however, the signal depends on subtle interplay of multiple molecular properties including potential energy surfaces of the ground and excited electronic states, or dependence of transition momenta on the geometry. Only recently, rigorous simulation methods were implemented.[15]

In spite of these challenges, RROA spectra proved useful in studying chiral nanotubes,[16] proteins,[11e] porphyrins[13a] other biomolecules,[17] and chiral metal complexes.[14b] For large proteins, for example, the RROA

spectroscopy can effectively increase the spatial resolution, preferentially collecting signal from vicinity of the chromophore.

We started to study the CoEDDS complex as a recommended standard material for chiral spectroscopy,[18] providing stability needed for RROA experiment. In addition, its relatively small size allows for thorough computational modeling. Similar chiral transition metal complexes are used as catalysts in organic synthesis,[19] coordinated cobalt itself is part of many enzymes.

Compared to the previously reported cases, the CoEDDS complex is rather exceptional in that the resonance with one electronic state is clearly apparent, the resonance leads to bisignate spectral pattern, and the experimental data can be reasonably well interpreted using ab initio models. The resonance behavior is very evident when Raman and RROA spectra are compared to those of the analogous aluminum complex (Figure 1). Above 1000 cm^{-1}, the Raman intensities of both compounds are comparable, and the 2950 cm^{-1} C–H stretching band cobalt is even smaller, possibly due to the absorption of the sample. Above 3000 cm^{-1}, the incompletely subtracted signal of water dominates. The higher background in *S*,*S*-CoEDDS Raman spectrum most likely comes from sample fluorescence. For Raman, the biggest difference is thus below 1000 cm^{-1}, where big bands appear for cobalt, up to six-times more intense than in the aluminum complex.

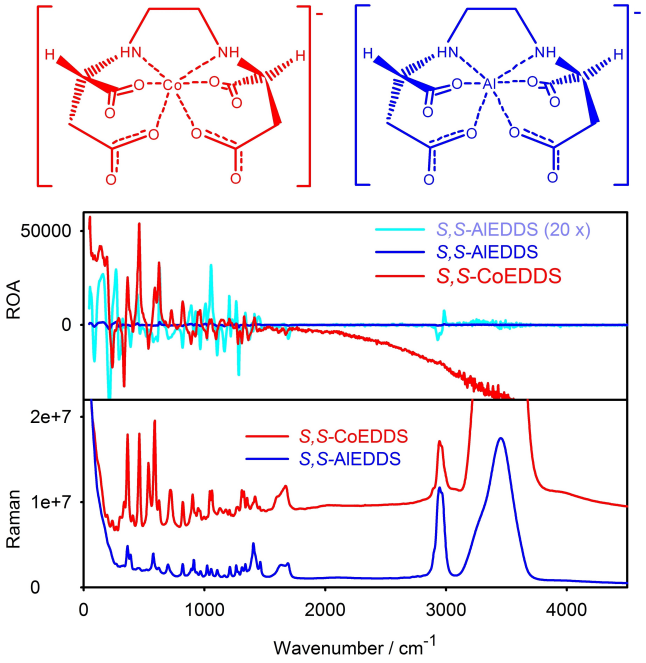

Figure 1. The Co(III) and Al(III) complexes with S,S-N,N-ethylenediaminedisuccinic anion (EDDS, top), and their SCP Raman and ROA spectra, bottom. The intensities are normalized to the excitation energy (laser power×time) and concentration. 20-times magnified S,S-AlEDDS ROA spectrum is shown as well. The resonance at CoEDDS is clearly manifested by stronger Raman and ROA signals below 1000 cm^{-1}.

The resonance effect is even more apparent in ROA intensities, also quickly rising for CoEDDS below 1000 cm^{-1}. The AlEDDS spectrum is almost invisible at the same scale! Except for the enhancement, the Raman band shapes of the two complexes are similar, while ROA patterns differ more, suggesting different underlying physical mechanisms. This can be also deduced from the so-called (normalized) circular intensity difference (CID, ROA/Raman ratio).[4,20] For the cobalt complex the typical value is about 5×10^{-3}; for the positive and negative bands around 200 cm^{-1} it even exceeds 10^{-2}. Such a high value has not been so far reported for ROA spectroscopy. For AlEDDS CID mostly remains below 2×10^{-3} (Figure S1).

The signal enhancement originates in a "borrowing" of the electronic chirality, subsequently manifested in the vibrational region.[10] This in general broadens the application span of ROA spectroscopy, allowing for shorter measurement times and smaller sample amounts.

Another experimental indication of the resonance can be obtained from the comparison of the SCP, DCP_I and DCP_{II} ROA spectra. These differ in modulation of the circularly polarized light, possible in an *ad hoc* experimental setup.[21] From the comparison in Table 1, it is clear that especially DCP_{II} ROA is a faithful indicator of resonance, being null otherwise. Non-zero DCP_{II} ROA can be viewed as a molecule behaving asymmetrically with respect to the incoming and scattered light.[22] Previously reported DCP_{II} bands were often debated as being artifacts.[23] To our knowledge, this is the first time when the signal is confirmed by a measurement of both enantiomers. Indeed, for CoEDDS they give "mirror images" of DCP_{II} ROA spectra (Figure S3). The strength of this signal is comparable to "normal" SCP ROA, thus also differing from the previous attempts when it was comparable to noise.

The bisignate character of all ROA spectra suggests that not only the Franck–Condon (related to the overlap between vibrational functions in the ground and excited electronic states), but also the Herzberg-Teller (changes of

Table 1: The three ROA experiments used: SCP, scattered circular polarization, DCP_I/DCP_{II}, dual circular polarization of the first/second kind.

Modulation	Incoming Light (upper index)	Analyzed Light (lower index)	Recorded Signal[a]	In Resonance	Off Resonance
SCP (default)	Unpolarized	Polarized	$I_R^u - I_L^u$	$\neq 0$	$= DCP_I$
DCP_I	Polarized	Polarized	$I_R^R - I_L^L$	$\neq 0$	= SCP
DCP_{II}	Polarized	Polarized	$I_L^R - I_R^L$	$= DCP_I$-SCP	0

[a] *L*/*R*/*u* for left/right/unpolarized light

dipole moments and other parameters during molecular vibrations) effect is involved.[4,15,20]

To confirm the quality of the chosen level of theory and understand the nature of the first excited electronic states of the cobalt complex, we measured and simulated its absorption and ECD spectra (Figure 2a, transitions parameters are listed in Table S1). The simulation reproduces well the experiment, and the third ($S_0 \rightarrow S_3$, note that the complex is closed-shell) transition is the closest one to the excitation wavelength. The transition electron density shows the substantial involvement of the *d*-orbitals (Figures 2b). Also the simplified Raman intensity contributions[4,20] of individual electronic transition (*I*, Figure 2c) confirm that the third one far outweighs all others with wavelengths longer than 300 nm. In the simulations presented below, the higher-energetic non-resonance transitions were nevertheless also added to the S_3 resonance polarizabilities as a perturbation (e.g., $\alpha = \alpha_{S3} + c\alpha_{NR}$, where c is arbitrary constant, see also SI). Because of the high density of states, their total contribution to the intensities may be important.[24] The effect of any transition may still be large, as exemplified in Figure 2c for transition number 26.

The usual far-from-resonance (FFR)[4] computation faithfully reproduces the experimental frequencies and intensities of AlEDDS (Figure 3). All methods tried (Figure S4) gave reasonable results; we found, for example, that MP2 and double-hybrid functionals slightly improved frequencies below 500 cm^{-1}, that changes with basis sets bigger than 6–311++G** were practically inexistent, and that anharmonic corrections in the fingerprint region (0–2000 cm^{-1}) did not bring any substantial improvement of the harmonic treatment. On the other hand, the explicit inclusion of water molecules was very beneficial to reproduce fine spectral patterns.

For the cobalt complex, however, the standard FFR approach failed (Figures S5, S6). Calculated CID ratios were too low and ROA intensities did not follow the experimental trends. These are better captured by the fully vibronic time-dependent (TD)[15,25] and sum-over-state (SOS)[22] models (Figure 4). Their variants still do not give signs or relative intensities of every band, but they reproduce the enhancement and relative intensity ratios of the ROA and Raman spectra. They all give reasonably well the ROA sign pattern between ≈300–600 cm^{-1}; the region below 300 cm^{-1} is dominated by unresolved strong hot bands, not included in the model. Above 600 cm^{-1}, contributions of the non-resonant polarizability parts prevail. The confrontation between theory and measurement thus leads us to a better understanding of the origin of the experimental intensities (Figures 4b and 4c).

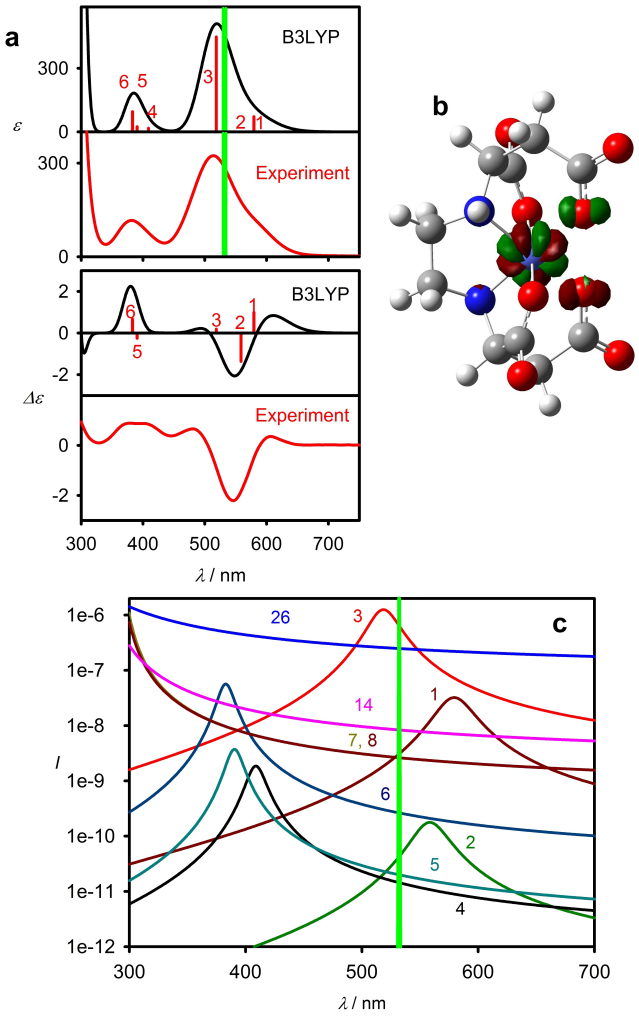

Figure 2. (a) Experimental and calculated (B3LYP/6–311++G**/6ek;CPCM(H_2O) absorption (***ε***) and ECD (***Δε***) spectra of S,S-CoEDDS, (b) transition electron density for the third transition, and (**c**) approximate contributions of electronic excited states to Raman intensities ($I = D^2 / |\omega - \omega_0 + i\Gamma|^2$, where *D* is the dipole strength, ω/ω_0 is the laser/transition frequency, $\Gamma = 500\ cm^{-1}$). The 532 nm excitation is indicated by the green line, the *I*-scale is logarithmic.

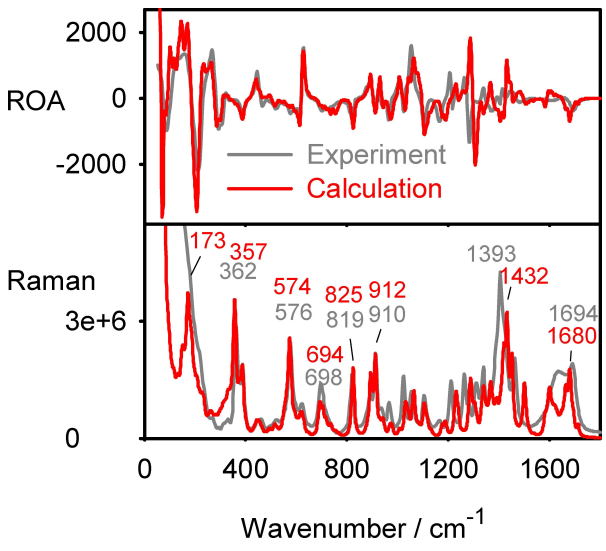

Figure 3. Experimental and calculated SCP ROA and Raman spectra of AlEDDS. The calculation was obtained at the B3LYP/6–311++G** /CPCM level as average of ten MD clusters with explicit water molecules.

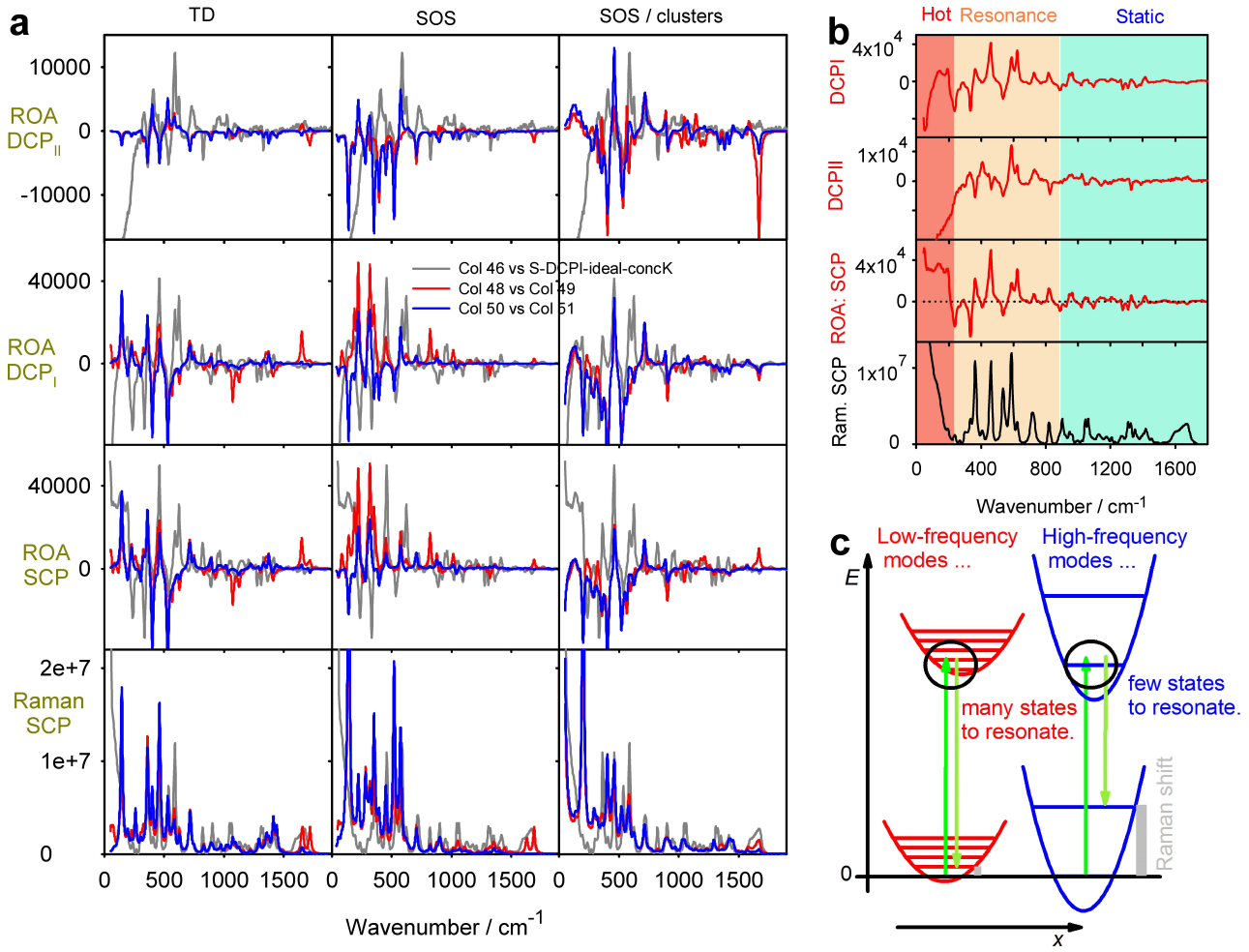

Figure 4. a) ROA (DCP_{II}, DCP_{I}, SCP) and SCP Raman spectra of CoEDDS calculated using the TD and SOS (SOS, with and without explicit waters) methods. Calculated spectra are normalized to SCP Raman areas within 250–1800 cm^{-1}. b) Experimental spectra approximately divided into three zones, with hot band, resonance and non-resonance scattering domination. **c**) Simplified Scheme of energy levels for low and high-frequency mode resonance.

Finally, the vibrational frequencies themselves provide interesting information about mechanical properties of the complexes. Internal force constants were constructed from the Cartesian force field[26] and verified by comparison of the calculated and experimental frequencies (Tables S2 and S3). The coordination bonds of CoEDDS and AlEDDS are shown side-by-side in Figure 5. We can see that in AlEDDS the strength of the three types of coordination bonds (metal - nitrogen, metal - main and side-chain oxygen) are quite uneven, the Al–N bond being the weakest. In CoEDDS, the bond strengths are closer to each other. As expected, the force constants indirectly correlate with the bond lengths (green in the Figure). These differences are reflected in the normal-mode vibrational motions and frequencies, although these do not change dramatically. The main differences in the spectra of the two molecules are thus caused by the different resonance conditions affecting only the intensities.

As a conclusion, for the first time, the antisymmetric chiral scattering signal (DCP_{II}) of the cobalt EDDS complex enantiomers could be observed, and the possibility to measure multiple ROA modulations provided detailed insight into chiral Raman scattering. The molecule exhibited an unusually strong Raman and ROA resonance, and most of the observed spectral features could be explained on the basis of vibronic quantum-chemical simulations. The $S_0 \rightarrow S_3$ electronic transition was identified as the main resonant response to the 532 nm laser radiation, although the single-state resonance was dominating only in the lower-frequency part of the spectra. The comparison with the colorless aluminum complex confirmed the sensitivity of the enhancement under resonance, illustrating possibilities of the resonance ROA spectroscopy for analytical chemistry and material industry.

Supporting Information

Raw spectra, computational details, band assignment, and details from the organic synthesis. The authors have cited additional references within the Supporting Information.[18,25–27]

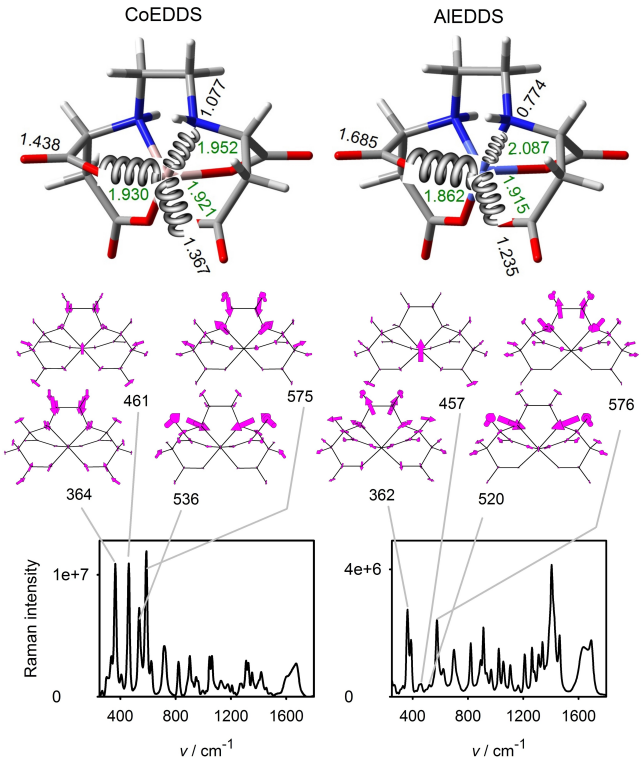

Figure 5. Geometry and mechanics of the cobalt (left) and aluminum (right) complexes, top: calculated coordination bond lengths (Å, green) and force constants (atomic units, black, spring sizes are proportional to them), bottom: experimental Raman spectra and selected vibrational normal modes with a high participation of the metal-nitrogen and metal-oxygen bond stretching.

Acknowledgements

The work was supported by the Grant Agency of the Czech Republic (22-04669S) and the Italian ministry of university and research (MUR), under the PRIN grant 2020HTSXMA "Photoreactive Systems upon Irradiation: Modelling and Observation of Vibrational Interactions with the Environment (PSI-MOVIE)".

Conflict of Interest

JK and JH are involved in commercialization of an ROA spectrometer. The other authors declare no conflict of interest.

Data Availability Statement

The data that support the findings of this study are available in the supplementary material of this article.

Keywords: Density Functional Theory · Metal Complexes · Raman Optical Activity · Resonance · Vibronic Theory

[1] C. V. Raman, *Indian J. Phys.* **1928**, *2*, 387–398.
[2] R. R. Jones, D. C. Hooper, L. Zhang, D. Wolverson, V. K. Valev, *Nanoscale Res. Lett.* **2019**, *14*, 231.
[3] L. D. Barron, M. P. Bogaard, A. D. Buckingham, *J. Am. Chem. Soc.* **1973**, *95*, 603–605.
[4] L. Nafie, *Vibrational optical activity: Principles and applications*, Wiley, Chichester, **2011**.
[5] a) P. L. Polavarapu, *J. Phys. Chem.* **1990**, *94*, 8106–8112; b) T. Helgaker, K. Ruud, K. L. Bak, P. Joergensen, J. Olsen, *Faraday Discuss.* **1994**, *99*, 165–180; c) K. Ruud, T. Helgaker, P. Bouř, *J. Phys. Chem. A* **2002**, *106*, 7448–7455.
[6] a) W. Hug, G. Hangartner, *J. Raman Spectrosc.* **1999**, *30*, 841–852; b) W. Hug, *Appl. Spectrosc.* **2003**, *57*, 1–13.
[7] a) F. J. Zhu, N. W. Isaacs, L. Hecht, L. D. Barron, *Structure* **2005**, *13*, 1409–1419; bT. A. Keiderling, *Chem. Rev.* **2020**, *120*, 3381–3419.
[8] M. Krupová, J. Kessler, P. Bouř, *ChemPlusChem* **2020**, *85*, 561–575.
[9] A. Ianoul, A. Mikhonin, I. K. Lednev, S. A. Asher, *J. Phys. Chem. A* **2002**, *106*, 3621–3624.
[10] G. Zając, P. Bouř, *J. Phys. Chem. B* **2022**, *126*, 355–367.
[11] a) L. A. Nafie, B. E. Brinson, X. Cao, D. A. Rice, O. M. Rahim, R. K. Dukor, N. J. Halas, *Appl. Spectrosc.* **2007**, *61*, 1103–1106; b) M. Unno, T. Kikukawa, M. Kumauchi, N. Kamo, *J. Phys. Chem. B* **2013**, *117*, 1321–1325; c) J. Kapitán, L. D. Barron, L. Hecht, *J. Raman Spectrosc.* **2015**, *46*, 392–399; d) Y. Zhang, P. Wang, G. Jia, F. Cheng, Z. Feng, C. Li, *Appl. Spectrosc.* **2017**, *71*, 2211–2217; e) S. Haraguchi, M. Hara, T. Shingae, M. Kumauchi, W. D. Hoff, M. Unno, *Angew. Chem. Int. Ed.* **2015**, *54*, 11555–11558; f) T. Fujisawa, R. L. Leverenz, M. Nagamine, C. A. Kerfeld, M. Unno, *J. Am. Chem. Soc.* **2017**, *139*, 10456–10460.
[12] L. A. Nafie, *Chem. Phys.* **1996**, *205*, 309–322.
[13] a) E. Machalska, G. Zajac, A. J. Wierzba, J. Kapitán, T. Andruniów, M. Spiegel, D. Gryko, P. Bouř, M. Baranska, *Angew. Chem. Int. Ed.* **2021**, *60*, 21205–21210; b) G. Li, J. Kessler, J. Cheramy, T. Wu, M. R. Poopari, P. Bouř, Y. Xu, *Angew. Chem. Int. Ed.* **2019**, *58*, 16495–16498; c) T. Wu, G. Li, J. Kapitán, J. Kessler, Y. Xu, P. Bouř, *Angew. Chem. Int. Ed.* **2020**, *59*, 21895–21898; d) G. Li, M. Alshalalfeh, W. Yang, J. R. Cheeseman, P. Bouř, Y. Xu, *Angew. Chem. Int. Ed.* **2021**, *60*, 22004–22009.
[14] a) E. Machalska, G. Zajac, A. Gruca, F. Zobi, M. Baranska, A. Kaczor, *J. Phys. Chem. Lett.* **2020**, *11*, 5037–5043; b) T. Wu, J. Kapitán, P. Bouř, *J. Phys. Chem. Lett.* **2022**, *13*, 3873–3877.
[15] A. Baiardi, J. Bloino, V. Barone, *J. Chem. Theory Comput.* **2018**, *14*, 6370–6390.
[16] M. Magg, Y. Kadria-Vili, P. Oulevey, R. B. Weisman, T. Bürgi, *J. Phys. Chem. Lett.* **2016**, *7*, 221–225.
[17] a) M. Vargek, T. B. Freedman, E. Lee, L. A. Nafie, *Chem. Phys. Lett.* **1998**, *287*, 359–364; b) M. Dudek, G. Zajac, A. Kaczor, M. Baranska, *J. Phys. Chem. B* **2016**, *120*, 7807–7814.
[18] A. Damianoglou, E. J. Crust, M. R. Hicks, S. E. Howson, A. E. Knight, J. Ravi, P. Scott, A. Rodger, *Chirality* **2008**, *20*, 1029–1038.
[19] a) Z. Dezhahang, M. R. Poopari, J. Cheramy, Y. Xu, *Inorg. Chem.* **2015**, *54*, 4539–4549; b) G. Wu, S. Wei, W. Ren, X. Lu, T. Xu, D. J. Darensbourg, *J. Am. Chem. Soc.* **2011**, *133*, 15191–15199.
[20] L. D. Barron, *Molecular Light Scattering and Optical Activity*, Cambridge University Press, Cambridge, UK, **2004**.
[21] P. Michal, R. Čelechovský, M. Dudka, J. Kapitán, M. Vůjtek, M. Berešová, J. Šebestík, K. Thangavel, P. Bouř, *J. Phys. Chem. B* **2019**, *123*, 2147–2156.
[22] L. Hecht, L. A. Nafie, *Mol. Phys.* **1991**, *72*, 441–469.

[23] a) G. S. Yu, L. A. Nafie, *Chem. Phys. Lett.* **1994**, *222*, 403–410; b) H. Li, L. A. Nafie, *J. Raman Spectrosc.* **2012**, *43*, 89–94; c) L. Hecht, D. Che, L. A. Nafie, *J. Phys. Chem.* **1992**, *96*, 4266–4270.

[24] a) K. B. Lipkowitz, T. R. Cundari, P. Elliot, F. Furche, K. Burke, in *Reviews in Computational Chemistry, Vol. 26* (Eds.: K. B. Lipkowitz, T. R. Cundari), John Wiley & Sons, Hoboken, New Jersey, **2009**, pp. 91–165; b) P. Štěpánek, P. Bouř, *J. Comput. Chem.* **2013**, *34*, 1531–1539.

[25] M. J. Frisch, G. W. Trucks, H. B. Schlegel, G. E. Scuseria, M. A. Robb, J. R. Cheeseman, G. Scalmani, V. Barone, B. Mennucci, G. A. Petersson, e. al, Wallingford Ct, **2022** Gaussian16 rev. C01.

[26] L. Benda, M. Straka, V. Sychrovský, P. Bouř, Y. Tanaka, *J. Phys. Chem. A* **2012**, *116*, 8313–8320.

[27] a) A. D. Becke, *J. Chem. Phys.* **1993**, *98*, 5648–5652; b) A. Klamt, G. Schuurmann, *J. Chem. Soc. Perkin Trans. 2* **1993**, 799–805; c) H. S. Yu, X. He, S. L. Li, D. G. Truhlar, *Chem. Sci.* **2016**, *7*, 5032–5051; d) T. Yanai, D. Tew, N. C. Handy, *Chem. Phys. Lett.* **2004**, *393*, 51–57; e) J. P. Perdew, K. Burke, Y. Wang, *Phys. Rev. B* **1996**, *54*, 16533–16539; f) C. Adamo, V. Barone, *J. Chem. Phys.* **1999**, *110*, 6158–6170; g) O. A. Vydrov, G. E. Scuseria, *J. Chem. Phys.* **2006**, *125*, 234109; h) Y. Zhao, D. G. Truhlar, *Theor. Chem. Acc.* **2008**, *120*, 215–241; i) L. E. Roy, P. J. Hay, R. L. Martin, *J. Chem. Theory Comput.* **2008**, *4*, 1029–1031; j) R. Salomon-Ferrer, D. A. Case, R. C. Walker, *Wiley Interdiscip. Rev.: Comput. Mol. Sci.* **2013**, *3*, 198–210; k) A. Spasic, J. Serafini, D. H. Mathews, *J. Chem. Theory Comput.* **2012**, *8*, 2497–2505; l) P. Bouř, T. A. Keiderling, *J. Chem. Phys.* **2002**, *117*, 4126–4132; m) J. R. Cheeseman, M. J. Frisch, *J. Chem. Theory Comput.* **2011**, *7*, 3323–3334; n) C. Møller, M. S. Plesset, *Phys. Rev.* **1934**, *46*, 618–622; o) S. Kozuch, J. M. L. Martin, *J. Comput. Chem.* **2013**, *34*, 2327–2344; p) F. Duschinsky, *Acta Physicochim. URSS* **1937**, *1937*; q) T. E. Sharp, H. M. Rosenstock, *J. Chem. Phys.* **1964**, *41*, 3453–3463; r) F. Santoro, FCClasses ver. 2.1, Istituto per i Processi Chimico-Fisici - CNR, Pisa, **2012**; s) J. A. Neal, N. J. Rose, *Inorg. Chem.* **1968**, *7*, 2405–2412; t) M. Oltmanns, A. Kirschning, *Synlett* **2020**, *31*, 1942–1946.

Manuscript received: August 25, 2023
Accepted manuscript online: September 20, 2023
Version of record online: October 2, 2023